

The 3D-QSAR analysis of 4(3H)-quinazolinone derivatives with dithiocarbamate side chains on thymidylate synthase

Shiying Liu,^{a,b,c} Feng Liu,^{a,b} Xiaoqing Yu,^d Guoyu Ding,^b Ping Xu,^c
Jian Cao^c and Yuyang Jiang^{a,b,*}

^aThe Key Laboratory of Chemical Biology, Guangdong Province, Graduate School at Shenzhen, Tsinghua University, Shenzhen 518055, China

^bKey Laboratory of Bioorganic Phosphorus Chemistry, Ministry of Education, Department of Chemistry, School of Life Science and Engineering, Tsinghua University, Beijing 100084, China

^cDepartment of Biological Engineering, Henan University of Technology, Zhengzhou 450052, China

^dShenyang Pharmaceutical University, Shenyang 110016, China

Received 26 July 2005; revised 25 September 2005; accepted 27 September 2005

Available online 2 November 2005

Abstract—Thymidylate synthase (TS) is a critical enzyme for DNA biosynthesis and many nonclassical lipophilic antifolates targeting this enzyme are quite efficient and encouraging as antitumor drug. In this paper, the binding model of 14 antifolates of 4(3H)-quinazolinone derivatives with dithiocarbamate side chains was examined using molecular simulation methods—FlexiDock and SCORE2.0. The resulted conformation and orientation of these antifolates were directly applied to CoMFA study. A good correlation between the calculated binding energies of these antifolates complexed with TS and their inhibitory activities was derived. The robust QSAR model, its three-dimensional contour map, and binding score for these antifolates derived from SCORE2.0 provided guidelines for structural optimization of current antifolates.

© 2005 Elsevier Ltd. All rights reserved.

1. Introduction

Thymidylate synthase (TS) catalyzes the reductive methylation of 2-deoxyuridine 5'-monophosphate (dUMP) to deoxythymidine 5'-monophosphate (dTMP) using the cofactor methylenetetrahydrofolate (CH₂THF) and provides the sole de novo means for synthesizing dTMP. TMP is required for DNA synthesis and inhibition of TS has proven to be an effective target for anticancer drug design. TS inhibition may be effected with quinazolinone-based compounds designed to occupy the cofactor site of the enzyme.¹ So structural modification of folic acid led to the discovery of a number of antifolates as efficient anticancer agents such as CB3717,^{1–3,7} ICI19583,¹ Tomudex,^{1–7} BW1843U89,⁷ etc. For example, Raltitrexed (Tomudex) has been registered widely for the first-line treatment of advanced colorectal cancer. However, these classical antifolates containing L-glutamic acid moiety in molecule have shortcomings

such as drug resistance and toxicity. One strategy to overcome these shortcomings is to design nonclassical lipophilic inhibitors of folate requiring enzymes by deleting or modifying L-glutamic acid component from the folate analogues.⁸ The cancer chemopreventive structure of dithiocarbamate moiety was incorporated into 4(3H)-quinazolinone. Our laboratory synthesized and found their in vitro antitumor activity. A series of 14 4(3H)-quinazolinone derivatives with dithiocarbamate side chains were employed in this study. To quantitatively disclose the relationship between activity and structure, 11 of these antifolates were selected as a training set with the aim of developing a 3D-QSAR (the quantitative structure–activity relationship, QSAR) model using CoMFA.

2. Materials and methods

2.1. Statistical parameters

Statistical parameters used during the development and validation of QSAR models will be discussed in this

Keywords: Thymidylate synthase; Antifolate; FlexiDock; QSAR.

* Corresponding author. Tel.: +86 755 2603 6840; fax: +86 755 26036029; e-mail: jiangyy@sz.tsinghua.edu.cn

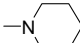
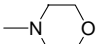
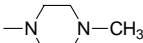
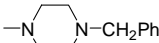
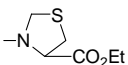
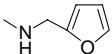
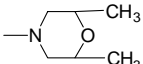
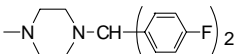
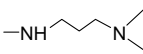
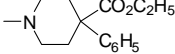
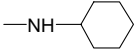
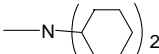
paper. R^2 is the correlation coefficient, calculated for both the training and test sets; q^2 is the leave-one-out cross-validated R^2 ; F and S^2 are the F value and the standard deviation of the regression, respectively.

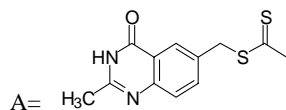
A series of 14 4(3*H*)-quinazolinone derivatives with dithiocarbamate side chains used in this study are listed in Table 1. Eleven of these compounds were selected as the training set, compounds labeled ^a serving as the test set for the validation of our model. The biological activity of each compound expressed as IC_{50} , which is the inhibitory concentration of compounds needed to inhibit 50% of K562 proliferation, was converted to pIC_{50} ($-\lg IC_{50}$) for the 3D-QSAR analysis. Their inhibitory activities shown as IC_{50} values were tested through the MTT ⁹ method within the same laboratory and by the same operator.

2.2. Molecular docking and alignment

Three-dimensional structure building and all modeling were performed using the Sybyl6.7 (Tripos Inc. 2001)¹⁰

Table 1. The structures of antifolates and their IC_{50} values

Compound	A-NR ₁ R ₂	IC_{50} (μM)
BZA	–NHCH ₂ Ph	4.0
PDQ	–N 	11.3
MOR	–N 	7.16
NMP	–N  –CH ₃	10.8
BZP ^a	–N  –CH ₂ Ph	7.43
DET ^a	–N(C ₂ H ₅) ₂	4.4
NSE	–N 	11
FUR	–N 	2.1
DMM	–N 	3.7
BFP	–N 	4.3
DMA	–NH 	25.6
PPE ^a	–N 	8.67
CHA	–NH 	31
DCH	–N 	7.6



^a These compounds are in the test set.

program package. The crystal structure of the complex of human TS with D16414 (ZD1694, Tomudex) was recovered from the Brookhaven Protein Data Bank (<http://www.rcsb.org/pdb/>) (entry code 1HVV). The potential of the 3D structure of TS was assigned according to the Tripos Force Field¹¹ with Kollman-all-atom¹² charges in Sybyl6.7. Energy minimization was performed using the Tripos Force Field with a distance-dependent dielectric and the Powell conjugate gradient algorithm with a convergence criterion of 0.05 kcal/mol Å. Partial atomic charges were calculated using Gasteiger–Hückel¹³ method.

It is well known that the selection of bioactive conformer and ascertainment of alignment rule are the most critical factors to the 3D-QSAR. In principle, the actual bioactive conformation and the best alignment can only be derived from the complex structure of ligand and receptor. So we performed a docking-guided conformation selection by FlexiDock^{14,15} in Sybyl6.7. Replacing the D16414 with these antifolates by extracting it from the complex, the initial active conformations of these antifolates were docked into the binding sites among the 3D-structural model of TS receptor. Then the docked ligands were subjected to perform flexible docking calculation employing the option of FlexiDock in Sybyl6.7. During our flexible docking calculation, all the single bonds of ligand and side chains of the amino acid residues around the ligand, as well as the orientation of the ligand, were taken as variables within the interaction region.

Thus, we obtained the initial structures of the ligand–receptor complexes, which were then successively refined using the option of minimization. The entire complex was minimized using 200 steps of steepest descent with a 0.05 kcal/mol Å energy gradient convergence criterion. The binding energy (E_{bind}) of the ligand was calculated using the following formula:

$$E_{\text{bind}} = E_{\text{complex}} - E_{\text{ligand}} - E_{\text{receptor}}, \quad (1)$$

where E_{ligand} is the energy of the ligand corresponding to the lower energy conformation and E_{receptor} is the energy of the receptor.

The conformer with the lowest binding energy was extracted from the docking result file and used for alignment. The molecular alignment was obtained by the Sybyl6.7 routine ‘Align Database’. D16414 was used as the alignment template and the rest of the molecules were aligned to it by using the common substructure labeled with* in Figure 1 for the CoMFA¹⁶ study.

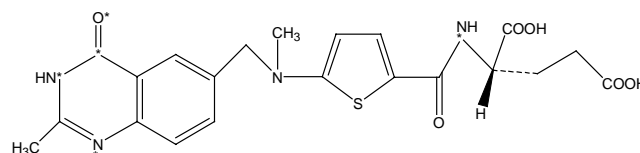


Figure 1. Template molecule D16414 (all molecules were aligned with atom *).

2.3. CoMFA and 3D-QSAR model

As for creating CoMFA column, steric and electrostatic field energies were calculated using an sp^3 carbon as the steric probe atom and a +1 charge for the electrostatic probe. Steric and electrostatic interactions were calculated using the Tripos force field with a distance-dependent dielectric constant at all intersections in a regularly spaced (2 Å) grid. Column filtering was set to 2.0 kcal/mol, to improve the signal-to-noise ratio by omitting those lattice points whose energy variation was below this threshold. Steric and electrostatic fields generated were scaled by the CoMFA-STD method in Sybyl6.7 with a default cutoff energy of 30.0 kcal/mol. The regression analysis was carried out using the partial least squares (PLS)¹⁷ method. The final model was developed with the optimum number of components equal to that yielding the maximal q^2 . The CoMFA descriptors were used as independent variables, and the pIC_{50} values were used as dependent variables in PLS regression analyses to derive the 3D-QSAR model using the standard implementation in the Sybyl6.7 package. The predictive value of model was evaluated first by leave-one-out (LOO) cross-validation. The cross-validated coefficient, q^2 , was calculated by using relative equations.¹⁸ CoMFA results may be extremely sensitive to a number of factors, such as alignment rules, overall orientation of aligned compounds, lattice shifting, step size, and probe atom type¹⁹. Cho et al. reported that q^2 value was sensitive to the orientation of aligned molecules on the computer terminal and might vary with the orientation by as much as 0.5 q^2 units.²⁰ So in our CoMFA analysis, all-orientation and all-placement searching was performed by rotating the molecular aggregates systematically every 30° along the *X*, *Y*, and *Z* axes and translating it every 0.2 Å, at every place, the cross-validated q^2 of PLS calculated, until obtaining a maximal q^2 value. For our investigated system, the maximal q^2 was obtained by translating aligned molecules 0.5 Å along the *X* axis.

2.4. Score

The 3D-structure of antifolates extracted from ligand–receptor complexes after FlexiDock was scored using SCORE2.0.^{21–23}

$$\begin{aligned} pK_d = & 2.254 + (0.916) \times MB - (0.168) \times VB \\ & + (0.141) \times WHB + (0.216) \times MHB \\ & + (0.593) \times SHB + (0.327) \times WWH \\ & - (0.708) \times MWH + (0.291) \times SWH \\ & + (1.178) \times HM - (0.169) \times RT. \end{aligned} \quad (2)$$

MB, coordinate bonding with metal ion; VB, VDW bump; WHB, weak H-bond; MHB, moderate H-bond; SHB, strong H-bond; WWH, weak water H-bond; MWH, moderate water H-bond; SWH, strong water H-bond; HM, hydrophobic matching; RT, rotatable single bond.

3. Result and discussion

3.1. Molecular docking

The active conformation of each antifolate was used to perform flexible docking calculation with the FlexiDock program of Sybyl6.7. We obtained 20 solutions for each antifolate after calculation. The complex with the lowest energy was chosen. The conformation and orientation of each antifolate were extracted from the complex for further study. The binding mode of 4(3*H*)-quinazolinone derivatives with dithiocarbamate side chains with receptor TS could be explained explicitly with the 3D-structure of these ligand–receptor complexes. In the 3D-structure of docked complexes, the quinazolinone and the lipophilic moieties of the 14 antifolates were in the hydrophobic groove formed by hydrophobic residues of TS, such as Phe80, Val79, Phe225, Gly83, Val84, Leu221, Asn226, Ile108, Met311, Pro224, Val313, His196, Gly222, and Leu192. Hydrogen bonding (Table 2) was the important intermolecular interaction. For example, FUR with the highest inhibitory activity, the distance between the N(2) of quinazolinone and CO of the residue Asn112 side chain (N–H···OC), NH₂ of the residue Asn112 side chain (N–H···N) was 2.259 and 2.384 Å, respectively, shown with a dashed line in yellow (Fig. 2). Since two hydrogen bonds were observed between the FUR and TS receptor, strong hydrogen bond interaction could be one of the reasons for the strong affinity with TS.

Table 3 is compiled with binding energy data of the 14 antifolate–receptor complexes. We performed a classical QSAR to explore whether the inhibitory activities of these antifolates could be correlated with the information of energy. Employing the PLS method of Sybyl6.7, we calculated the regression equation for the inhibitory activities (pIC_{50}), using the binding energies E_{bind} as the sole descriptor variable. A perfect correlation was found between the inhibitory activities and binding energies (Eq. 3),

$$pIC_{50} = -0.002 + 0.001E_{\text{bind}}, \quad (3)$$

which is an indirect proof for the reasonability of the 3D-structure of ligand–receptor complexes predicted by our modeling methods.

3.2. 3D-QSAR model and CoMFA analysis

Eleven of fourteen antifolates constitute the training set, the rest labeled ^a the test set. The aligned molecular aggregates are shown in Figure 3. A QSAR model was

Table 2. Hydrogen bonding between these antifolates and TS

Compound	Receptor (No.)	Residue	Donor (No.)	Distance (Å)	Angle (°)
BFP	F(54)	Trp109	–NH	1.415	141.06
DCH	O(1)	Asn226	–NH ₂	2.427	154.29
FUR	N(2)	Asn112	–NH ₂	2.384	138.23
Asn112	CO	FUR	–NH(2)	2.259	120.50
MOR	N(3)	Asn112	–NH ₂	2.624	158.52
NSE	O(30)	Met311	–NH ₂	2.740	134.52

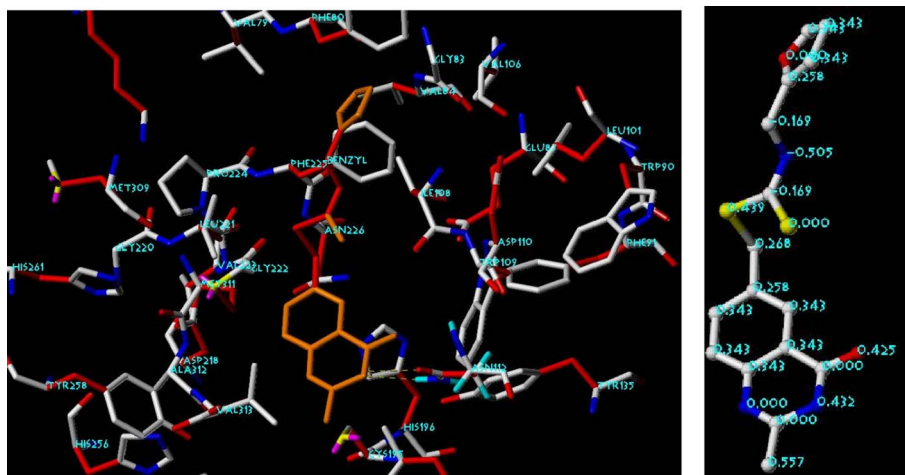


Figure 2. 3D structure of the FUR complex with TS and the binding score of FUR. Left, FUR complex with TS (two hydrogen bonds shown with a dashed line in yellow); right, binding score of FUR.

Table 3. Binding energy of 14 antifolate–receptor complexes

Compound	ΔE (kcal/mol)
BFP	−424.54
BZA	−420.66
BZP	−379.25
CHA	−434.07
DCH	−383.52
DET	−406.22
DMA	−398.34
DMM	−411.17
FUR	−423.15
MOR	−461.10
NMP	−419.18
NSE	−429.51
PDQ	−440.87
PPE	−418.12

Table 4. The result of CoMFA analyses

Cross-validation		Non-cross-validation		
Rcross ²	Component	r^2	s	F
0.563	3	0.964	0.081	63.250

obtained using the methods of docking-guided conformer selection and all-orientation and all-placement searches. The PLS statistics of the CoMFA analyses are summarized in Table 4. The cross-validated q^2 value was 0.563 with 3 components and noncross-validated conventional r^2 value was 0.964 with a standard error of estimate (SEE) value of 0.081. The relative contribution between steric and electrostatic field for the CoMFA model was 0.606 and 0.394, respectively.

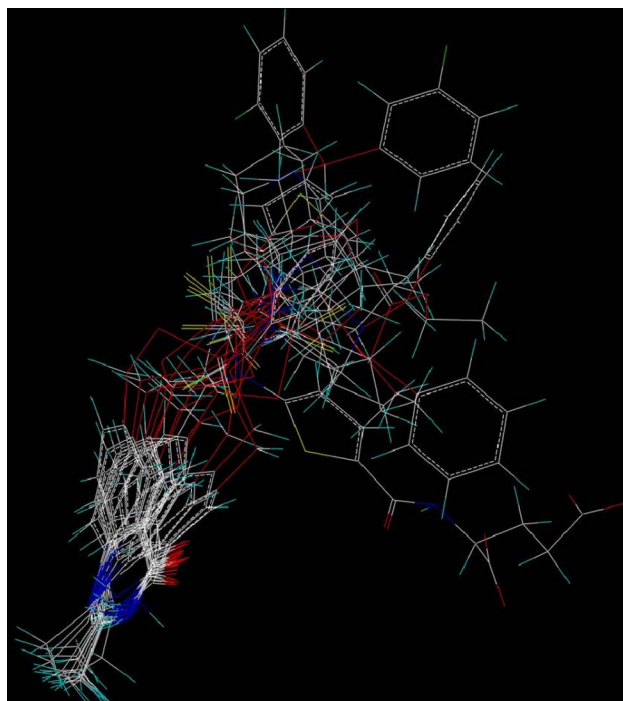


Figure 3. Alignment of the antifolates.

The contours of the steric and electrostatic fields were displayed. The steric contours (Fig. 4) are displayed in yellow and green and the electrostatic contours (Fig. 5) in red and blue. The meanings of the different colors are shown in the caption of the figure. Comparing compounds DCH, DET with DMA, CHA, it can be seen that compounds containing a secondary amine moiety have activities stronger than those containing primary amine moiety. Compounds containing benzyl or furfuryl primary amine moiety (BZA and FUR) have strong activities. Compound PPE has activities stronger than those PDQ, also suggesting that the introduction of an aryl group into amino moiety resulted in the enhancement of activity. When the oxygen atom (negative charge) was introduced into the piperidine ring, the resulting compounds MOR and DMM were more active than the parent compound PDQ. Compounds BZP and BFP having an aryl or arylalkyl group at the 4-position of piperazine ring have stronger activities than NMP with methyl at 4-position of piperazine ring.

3.3. Validation of the QSAR Models

To test the stability and predictive ability of the 3D-QSAR model, 3 antifolates, which were not included

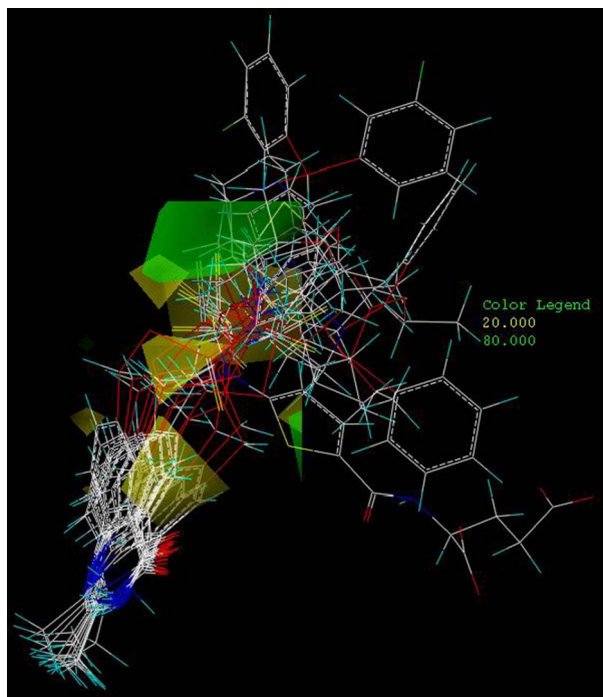


Figure 4. The steric field contours of the QSAR model. The yellow contours indicate regions of negative steric potential, while the green contours indicate regions of positive steric potential.

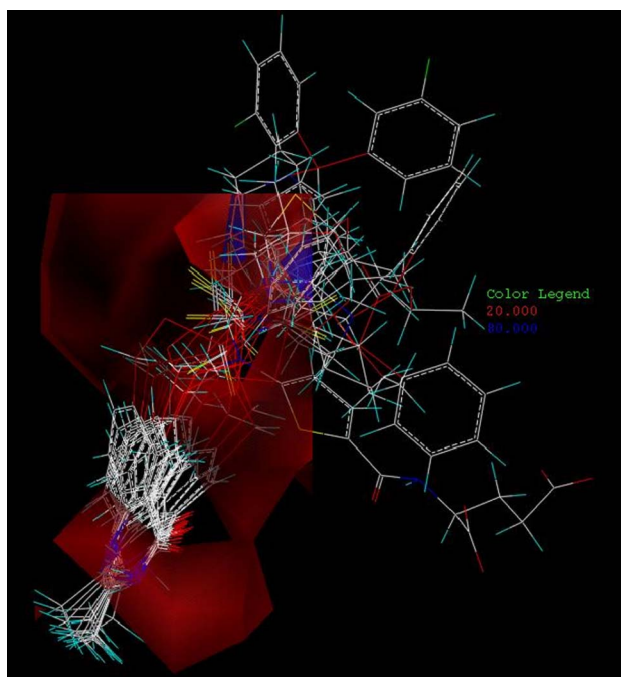


Figure 5. The electrostatic field contours of the QSAR model. The red contours indicate regions of negative electrostatic potential and the blue contours indicate regions of positive electrostatic potential.

in the CoMFA models, were selected as a set for validation. The residual between experimental and predicted pIC_{50} for this test set is listed in Table 5. The correlation between experimental and predicted pIC_{50} for training set is shown in Figure 6. It was shown that the model was stable and had robust predictive ability.

Table 5. Residuals of the predicted pIC_{50} in the test by the CoMFA model

Compound	Actual	Predict	Residue
*BZP	2.13	2.06	0.07
*DET	2.36	2.28	0.08
*PPE	2.06	2.13	−0.07

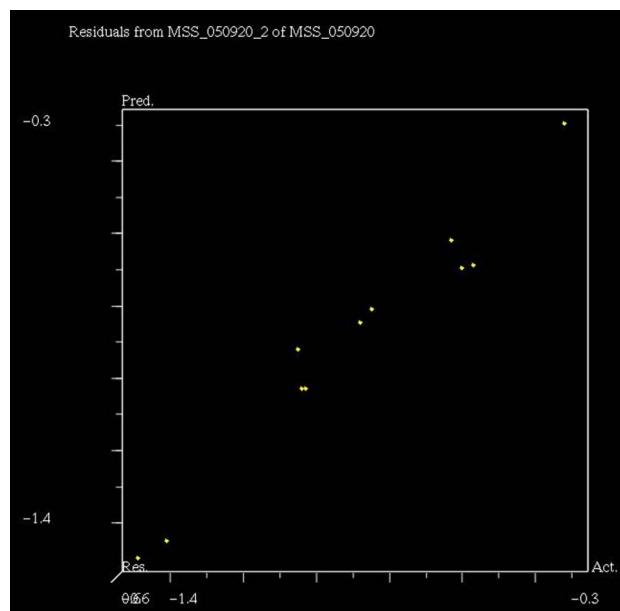


Figure 6. Predicted versus experimental inhibitory activities for training set.

3.4. Score

Performing scoring for every antifolate within the docked complex, we obtained a score for every atom of every antifolate and assessed the contribution of every atom to interaction between antifolates and TS. The atoms, which score above 0.1, were favorable for the interaction, below −0.1 unfavorable. The common favorable atoms of these 14 antifolates were phenyl moiety of quinazolinone and connected CH_3 , C, and S. For example, atom codes 1, 2, 4, 5, 6, 7, 8, 9, 12, 15, 21, 26, 27, 28, and 29 were favorable for interaction between FUR and TS. 3, 10, 11, and 24 were neutral, and 22, 23, and 25 were unfavorable as shown in Figure 2.

4. Conclusion

We applied FlexiDock, CoMFA, and SCORE2.0 to research the binding mode of a set of antifolates to TS receptor. Through docking the antifolates with the TS receptor, hydrogen bonds between antifolates and the residues of TS were discovered. FlexiDock results indicate that the binding free energies of the antifolates correlate well with the experimental inhibitory activities against TS, and the modeling results provided a satisfactory explanation for the binding mode of these antifolates with TS. The probable conformations were selected by the docking-guided conformer selection

method, and then the 3D-QSAR model was created by the method of all-orientation and all-placement, whose statistical parameter (PLS) was ideal. The structures of these antifolates were cancer chemopreventive structure of dithiocarbamate moiety incorporated into 4(3*H*)-quinazolinone. The score of dithiocarbamate moiety of these antifolates was 0.493, which was higher than that of the corresponding structure of D16414 by using SCORE2.0. Inhibitory activities (IC₅₀) of many of these antifolates were within 10 μM, the incorporated dithiocarbamate moiety was favorable for interaction between these antifolates and TS. The introduction of dithiocarbamate moiety into 4(3*H*)-quinazolinone was an excitement for antifolate design.

Understanding protein–ligand interactions is essential for designing novel synthetic candidates, while those interactions are difficult to describe. 3D-QSAR results based on CoMFA allow focus on those regions, where steric and electrostatic effects play a dominant role in ligand–receptor interactions. In this study, we combined the results of 3D-QSAR with SCORE2.0, which leads to a better understanding of important protein–ligand interactions and thus provided guidelines for ligand design plus a predictive model for scoring novel synthetic candidates. They could help us design new and higher activity antifolates.

Acknowledgment

This work was supported by the National Natural Science Foundation of China (Grant No. 20472043).

References and notes

- Jonathan H. Marriott; Stephen Neidle; Zbigniew Matysiak; Vassilios Bavetsias; Jackman, Ann L.; Camille Melin; Thomas Boyle, F. J. Chem. Soc., Perkin Trans. **1999**, 1, 1495.
- Kelland, L. R.; Kimbell, R.; Hardcastle, A.; Aherne, G. W.; Jackman, A. L. *Eur. J. Cancer* **1995**, 31A, 981.
- Jackman, A. L.; Farrugia, D. C.; Gibson, W.; Kimbell, R.; Harrap, K. R.; Stephens, T. C.; Azab, M.; Boyle, F. T. *Eur. J. Cancer* **1995**, 31A, 1277.
- Peters, Godefridus J.; Smitskamp-Wilms, Evelien; Smid, Kees; Pinedo, Herbert M.; Jansen, Gerrit *Cancer Res.* **1999**, 59, 5529.
- Lewis, Nancy L.; Scher, Richard; Gallo, James M.; Engstrom, Paul F.; Szarka, Christine E.; Litwin, Samuel; Adams, Andrea L.; Kilpatrick, Deborah; Brady, Diane; Weiner, Louis M.; Meropol, Neal J. *Cancer Chemoth. Pharm.* **2002**, 50, 257.
- Bavetsias, Vassilios; Clauss, Rainer; Henderson, Elisa A. *Org. Biomol. Chem.* **2003**, 1, 1943.
- McGuire, John J. *Curr. Pharm. Des.* **2003**, 9, 2593.
- Cao, Sheng-Li; Feng, Yu-Ping; Jiang, Yu-Yang; Liu, Shi-Ying; Ding, Guo-Yu; Li, Run-Tao *Bioorg. Med. Chem. Lett.* **2005**, 15, 1915.
- Mosmann, T. *J. Immunol Methods* **1983**, 65, 55.
- Tripos Associates, St. Louis. Mo. Sybyl. version 6.7, 1998.
- Clark, M.; Cramer, R. D., III; Van Opdenbosch, O. N. *Tripos Force Field J. Comput. Chem.* **1989**, 10, 982–1012.
- Weiner, S. J.; Kollman, P. A.; Case, D. A.; Singh, U. C.; Ghio, C.; Alagona, G.; Profeta, S., Jr.; Weiner, P. *J. Am. Chem. Soc.* **1984**, 106, 765.
- Tripos: St. Louis, MO, Details of the implementation are given in Sybyl6.5 Theory Manual; 1998, 69.
- Tripos Inc. 1699 South Hanley Rd, St. Louis, MO, USA. Sybyl6.5 Manual; 1999.
- Judson R. In: Lipkowitz, K. B., Boyd, D. B., (Eds.). *Rev. Comp. Ch.*, vol. 10. New York: VCH Publishers, 1997.
- Cramer, M.; Cramer, R. D., III; Jones, D. M. *J. Am. Chem. Soc.* **1988**, 110, 5959–5967.
- Stahle, L.; Wold, S.; Ellis, G. P.; West, G. B. (Eds.), Elsevier; 1988, p. 292–338.
- Andrew, R. L. *Molecular modeling Principles and Applications*; Henry Ling Ltd Press, 2001, 695–702.
- Cho, S. J.; Tropsha, A. *J. Med. Chem.* **1995**, 38, 1060–1066.
- Cho, S. J.; Tropsha, A. *J. Med. Chem.* **1995**, 38, 1060–1066.
- Wang, Renxiao; Liu, Liang; Lai, Luhua; Tang, Youqi. *J. Mol. Model* **1998**, 4, 379.
- LI, Chun-hua; MA, Xiao-hui; CHEN, Wei-zu; WANG, Cum-xin. *Acta Biophysica. Sinica* **2003**, 19, 47.
- LIU, Liang; WANG, Xiaoren; LAI, Luhua; LI, Chongxi. *Acta Phys.-Chim. Sin.* **1997**, 13, 1090.